https://doi.org/10.3311/PPch.37876

Periodica Polytechnica Chemical Engineering, 69(1), pp. 149–162, 2025

Mechanical, Morphological, and Electrical Properties of Polylactic Acid-based Conductive Polymer Composites through Polyethylene Glycol and Carbon Nanotubes Integration

Awaludin Fitroh Rifa'i[1], Mujtahid Kaavessina[1*], Sperisa Distantina[1]

[1] Department of Chemical Engineering, Faculty of Engineering, Universitas Sebelas Maret, Jalan Ir. Sutami 36A, 57126 Surakarta, Indonesia
[*] Corresponding author, e-mail: mkaavessina@staff.uns.ac.id

Received: 12 July 2024, Accepted: 27 November 2024, Published online: 11 March 2025

Abstract

Polylactic acid (PLA) is a biodegradable aliphatic polymer obtained from renewable sources, primarily used in the packaging sector. Electronic components require antistatic packaging to prevent electrostatic discharge (ESD). PLA, being non-conductive, necessitates the addition of conductive carbon nanotube (CNT) to reduce its resistivity and make it suitable for antistatic packaging applications. This research investigates the effect of polyethylene glycol (PEG) on the properties of conductive polymer composites (CPCs) based on PLA, using solvent casting to form film sheets. Four different concentrations of PEG-1,000 and PEG-10,000 (0, 6, 10, and 14 wt%) were utilized to improve the ductility of PLA. CNT was incorporated at a concentration of 8 wt% to enhance the mechanical and electrical properties of PLA. The addition of PEG to the PLA/CNT composites resulted in a reduction in tensile strength while increasing elongation at break, thereby indicating improved flexibility. FTIR analysis revealed significant changes in the carbonyl group peak at 1747 cm^{-1}, with a decrease in carbonyl content observed as the concentration and molecular weight of PEG increased. The electrical conductivity of the CPCs showed a notable increase with the incorporation of 14 wt% PEG, rising from 1.89×10^{-11} S cm^{-1} to 5.62×10^{-8} S cm^{-1} (PEG-1,000) and 1.25×10^{-7} S cm^{-1} (PEG-10,000). These results demonstrate that PEG enhances the mechanical flexibility and electrical conductivity of PLA/CNT composites, making them promising candidates for antistatic packaging applications.

Keywords

conductive polymer composite, carbon nanotubes, polyethylene glycol, polylactide acid, solvent casting

1 Introduction

Electrostatic discharge (ESD) is a key problem that causes losses in products containing sensitive electronics during manufacturing, assembly, storage, and shipping [1]. To mitigate this issue, it is essential to use antistatic agents that impart dissipative properties to these materials, allowing for the conduction of electrons through their structures. Conducting polymers, particularly those based on inorganic or metal particle-filled composites, are versatile materials widely applied in electronic devices, including Antistatic and dissipative materials [2].

There are four main types of polymers that conduct electricity:

1. inherently conducting polymers (ICPs),
2. polymer charge transfer complexes,
3. organometallic polymer conductors,
4. conductive polymer composites (CPCs) [3].

CPCs, which combine conductive fillers with insulating polymer matrices, have found widespread applications in electronic devices, batteries, fuel cells, heat sinks, electromagnetic shielding, and antistatic packaging [4–7]. However, the accumulation of electronic waste (white pollution) and the depletion of petroleum resources highlight the need for biodegradable and renewable CPCs [8]. Dispersing electrically conductive fillers or ICPs in an insulating polymer matrix, such as thermosets or thermoplastics, creates CPCs. Achieving the desired level of electrical conductivity depends on the specific application. Conductive fillers commonly used include carbon black (CB), graphite, metal particles, carbon nanotubes (CNTs), graphene, expanded graphite (ExGr), and carbon nanofibers (CNFs) [1, 3, 8].

Polylactic acid (PLA) is a biodegradable polyester that has garnered significant interest due to its potential appli-

Cite this article as: Rifa'i, A. F., Kaavessina, M., Distantina, S. "Mechanical, Morphological, and Electrical Properties of Polylactic Acid-based Conductive Polymer Composites through Polyethylene Glycol and Carbon Nanotubes Integration", Periodica Polytechnica Chemical Engineering, 69(1), pp. 149–162, 2025. https://doi.org/10.3311/PPch.37876

cations across various industries, including biomedical, food packaging, composites, automotive, and electronics. However, PLA's brittleness, hydrophobicity, low melt strength, low heat resistance, slow degradation rate, and crystallization kinetics limit its broader application [9, 10]. To enhance PLA as a CPCs, its mechanical properties and electrical conductivity need improvement.

Several modification techniques can tailor PLA properties, such as copolymerization, blending, plasticization, and the incorporation of fillers [11]. Among these, the blending technique is advantageous due to its simplicity and cost-effectiveness compared to copolymer synthesis. By adjusting the component ratio in polymer blends, a broad range of mechanical properties and degradation rates can be achieved [10].

Blending methods include melt blending and solvent casting. Melt blending involves heating the polymer to its melting temperature and mixing it with other polymers or fillers under these conditions. Solvent casting, based on Stokes' law, dissolves each polymer in a suitable solvent before combining them in solution. Filler dispersion in this method is achieved in the solution phase, often aided by stirring or ultrasonic homogenization, resulting in superior and uniform dispersion of blends [12].

Carbon nanotubes are now applied as conductive fillers because of their excellent electrical conductivity (10^3–10^5 S cm^{-1}) [13, 14]. CNTs also enhance the mechanical properties of polymer blends, with increased CNT concentration correlating with higher tensile modulus and tensile strength in PLA/CNT composites [15]. Moreover, the electrical resistivity of the polymer blend decreases significantly with the addition of CNTs, suggesting applications such as antistatic packaging [1]. Uniform dispersion of CNTs within the matrix is crucial to maximizing conductivity, as inadequate dispersion yields minimal conductivity improvement [16].

Incorporating multi-walled carbon nanotubes (MWCNTs) into the PLA matrix has produced composites with electrical conductivities up to 1.13 S cm^{-1} [17]. The uniform dispersion of MWCNTs enhances the tensile strength and elastic modulus of PLA, although elongation and flexibility decrease as the nanoparticle composition increases. Improving these properties is essential for broader PLA applications, given its inherent brittleness [18]. Introducing polyethylene glycol (PEG) as a plasticizer can mitigate some of PLA's limitations. The addition of PEG to the PLA matrix has been shown to increase elongation at break while decreasing tensile strength and elastic modulus [19]. PLA and PEG blends also demonstrate excellent miscibility and biodegradability [11].

The counterintuitive influence of CNT fillers and PEG plasticizers on the mechanical properties of PLA underscore the need for a comprehensive exploration of their combined effects to advance PLA as a conductive polymer composite. Notably, the impact of various PEG molecular weights on the electrical conductivity and morphological properties of PLA/CNT composites remains underexplored. In this study, we address this gap by synthesizing PLA composites with CNT and PEG using the solvent casting method. We investigate the role of PEG by varying its concentration and molecular weight (1,000 and 10,000 Da). Qualitative analysis using Fourier transform infrared (FTIR) spectroscopy examines the potential functional group interactions, the structural polymorphs, and the crystallinity index within the PLA matrix due to CNT and PEG inclusion. Scanning electron microscopy (SEM) assesses the morphology of the CPCs, focusing on CNT dispersion within the matrix. Furthermore, we characterize the mechanical and electrical properties to determine the impact of PEGs on the performance of the PLA/CNT composite.

2 Materials and methods

2.1 Materials

Commercial PLA from Xiamen Keyuan Plastic was used as the matrix material, which has a density of 1.25 g cm^{-3}, a glass transition temperature (T_g) of approximately 60 °C, and a melting temperature (T_m) of 170 °C. MWCNTwas obtained from Jiangsu XFNANO Materials with an average diameter of 20–30 nm, length of 0.5–2 μm, purity of up to 95%, and electrical conductivity of approximately 100 S cm^{-1}. PEG with two different molecular weights (M_w) (1,000 and 10,000 Da) and analytical grade chloroform were purchased from Sigma–Aldrich. All chemicals were applied without any prior purification.

2.2 Composite preparation

By solvent casting, neat PLA and its composites were created into film sheets. Before processing, PLA was dried overnight in an oven at 80 °C to remove moisture content. According to the fabricating steps in Fig. 1, PLA was dissolved in 10 mL chloroform and stirred using a magnetic stirrer at 150 rpm and 55 °C for approximately 1 h. CNT with a composition of 8 wt% CNT was also dispersed in 2 mL chloroform using an ultrasonic tip (Kingqi Science Model: KQJS-800, (P = 800 W; amplitude = 40%), for 30 min. An ultrasonic homogenizer was used to disrupt the van der

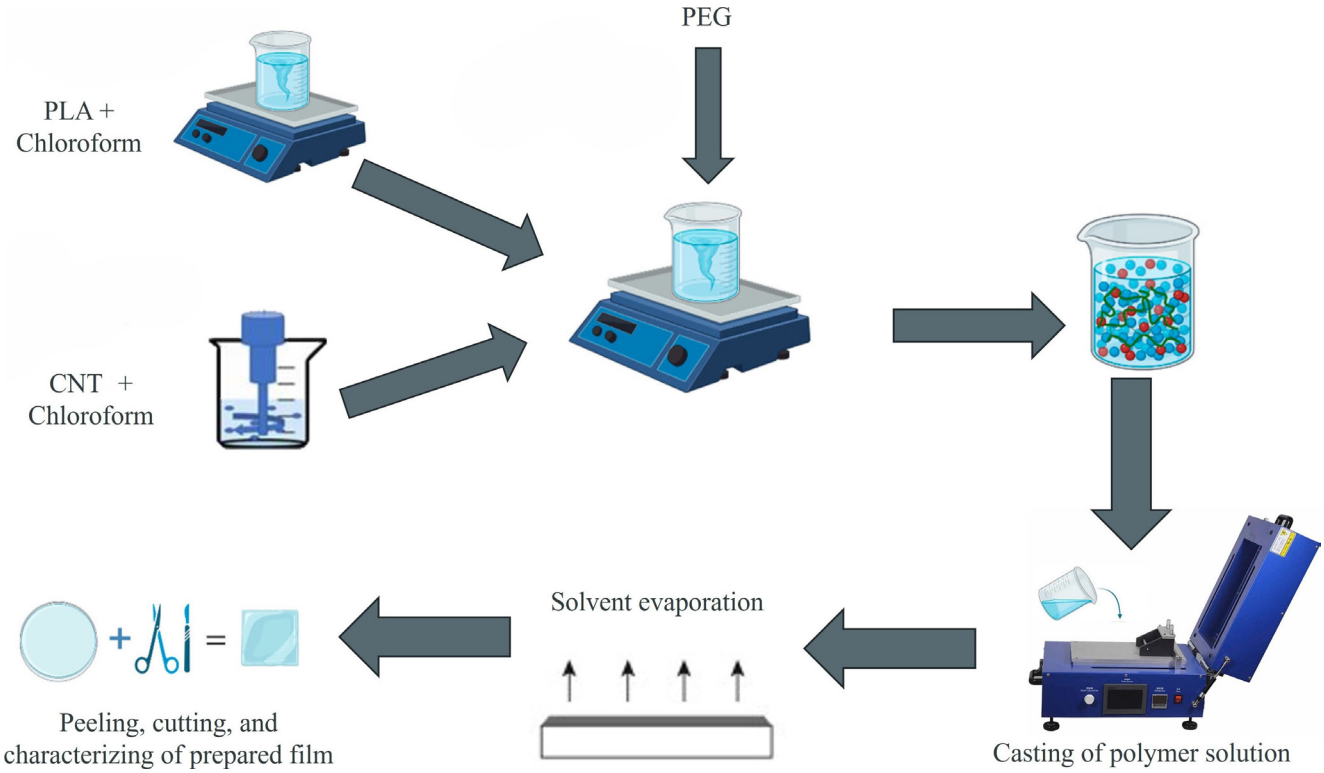

Fig. 1 Preparation procedures for the PLA and CPCs

Waals forces between particles, which caused the agglomeration tendency of the nanosized particles. Four different loadings of PEG (0, 6, 10, and 14 wt%) were prepared as plasticizers to enhance the ductility, toughness, and flexibility of PLA. Then, these three chemicals (PLA solution, dispersed CNT, and PEG) were mixed and stirred for 30 min. The obtained solution was then poured into a film machine (TMAX-TCC1, Xiamen Equipment, China) with a filling velocity of 1 mm s^{-1}. The filling velocity of 1 mm s^{-1} was selected based on preliminary trials and previous studies that indicated it provided optimal dispersion of the CNT within the PLA matrix without inducing shear-related degradation or agglomeration of the CNT. The composition of CNT and PEG added to the PLA solution and the nomenclature of the samples are described in Table 1.

Table 1 List of the PLA/CNT/PEG composite samples prepared

Sample	M_w of PEG (Da)	PLA (wt%)	CNT (wt%)	PEG (wt%)
PLA	–	100	0	0
PLA/CNT	–	92	8	0
PLA/CNT/PEG6 (1)	1,000	86	8	6
PLA/CNT/PEG10 (1)	1,000	82	8	10
PLA/CNT/PEG14 (1)	1,000	78	8	14
PLA/CNT/PEG6 (10)	10,000	86	8	6
PLA/CNT/PEG10 (10)	10,000	82	8	10
PLA/CNT/PEG14 (10)	10,000	78	8	14

2.3 Mechanical characterization

The mechanical properties of neat PLA and its composites were evaluated by tensile tests. The tensile test was carried out in a universal tensile testing machine (Lyxyan HZ-1007A, China) at ambient temperature with a crosshead speed of 1 mm min^{-1}, according to the ASTM D882-10 standard [20]. The thickness of the molded ASTM samples was previously measured by a digital caliper (Krisbow KW06-351). The thickness and gauge length were prescribed to be 0.04–0.1 mm and 50 mm, respectively. Three specimens of each sample were examined at room temperature to obtain average data.

2.4 Fourier transform infrared (FTIR) spectroscopy

The functional groups of neat PLA and its composites were confirmed using attenuated total reflectance-Fourier transform infrared (ATR-FTIR) spectroscopy (Ir-Spirit FTIR, Shimadzu). The films were scanned using infrared radiation with wavenumbers in the range of 400–4000 cm^{-1}. FTIR was also employed to examine the structural polymorphs of PLA, focusing on the intensity ratios of specific absorption bands. The intensity ratios $I_{1384/1361}$ and $I_{1211/1186}$ were used to quantitatively assess structural alterations in PLA and CPCs. The values of $I_{1384/1361}$ and $I_{1211/1186}$ were calculated according to the Eqs. (1) and (2) [21, 22]:

$$I_{1384/1361} = \frac{A_{1384}}{A_{1361}} = \frac{2 - \log(T\%)_{1384}}{2 - \log(T\%)_{1361}}, \quad (1)$$

$$I_{1211/1186} = \frac{A_{1211}}{A_{1186}} = \frac{2 - \log(T\%)_{1211}}{2 - \log(T\%)_{1186}}, \quad (2)$$

with A_{1384}, A_{1361}, A_{1211}, and A_{1186} referring to the absorbance at 1384, 1361, 1211, and 1186 cm^{-1} bands, respectively. The $T\%$ indicates the percent of transmittance at the respective band. To further assess crystallinity, we followed the method outlined by Giełdowska et al. [23], measuring the absorbance at the 921 and 957 cm^{-1} bands to determine the crystallinity index using Eq. (3):

$$x_{IF} = \frac{A_{921}}{A_{921} + A_{957}} \times 100\%, \quad (3)$$

where x_{IF} represents the overall crystallinity index, A_{921} and A_{957} determine the total absorption of the bands at 921 and 957 cm^{-1}, respectively.

2.5 Morphological characterization

The distribution morphology of the nanoparticles (CNT) in the conductive polymer composites was observed using scanning electron microscopy (SEM) (SEM-EDX JEOL JSM 6510LA, Japan). This SEM instrument was preinstalled with energy-dispersive X-ray spectroscopy (EDX). The film sheets of the samples were coated with a thin layer of gold, and then, the surface was examined by SEM at 20 kV and 1,000× magnification.

2.6 Electrical conductivity

The electrical volume resistivity (ρ_v) of the conductive polymer composites was determined by measuring at room temperature and ambient humidity using a ZC-90G insulation resistance tester. The setup is schematically depicted in Fig. 2. The volume resistance (R_v (Ω)) obtained from this measurement was then converted to the electrical ρ_v (Ω cm) using Eq. (4). Additionally, the electrical conductivity of the samples was calculated from the resistivity values using Eq. (5) [24, 25]:

$$\rho_v = R_v \times \frac{A}{h}, \quad (4)$$

$$\sigma = \frac{1}{\rho_v}, \quad (5)$$

where A is the effective area of the measuring electrode (21.24 cm^2), h is the average thickness of the sample (cm), and σ is the electrical conductivity (S cm^{-1}). The average electrical conductivity data were the result of measurements on three specimens for each sample.

3 Results and discussions

3.1 Tensile properties

The influence of the addition of CNT and PEG on the tensile properties of the PLA composites is discussed in this section. Fig. 3 (a) shows typical stress-strain curves from the tensile test for neat PLA and its composites. It illustrates the changes in the mechanical behavior of the samples caused by the addition of PEGs. The mean values of the mechanical properties obtained from the stress-strain curves are shown in Fig. 3 (b), (c), and (d).

Neat PLA is characterized by its rigidity, brittleness, and tendency to fracture near the yield point, consistent with other reported PLA results [19, 26]. PLA typically shows low elongation at break, high tensile strength, and a high tensile modulus. Specifically, neat PLA demonstrates an elongation at break of approximately 4.2%, a tensile strength of around 23.747 MPa, and a tensile

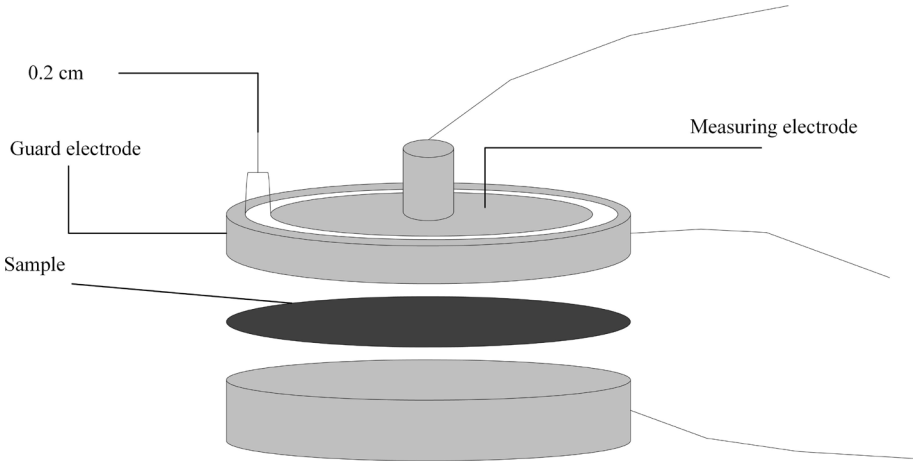

Fig. 2 Schematic setup for the ρ_v measurement of the composites

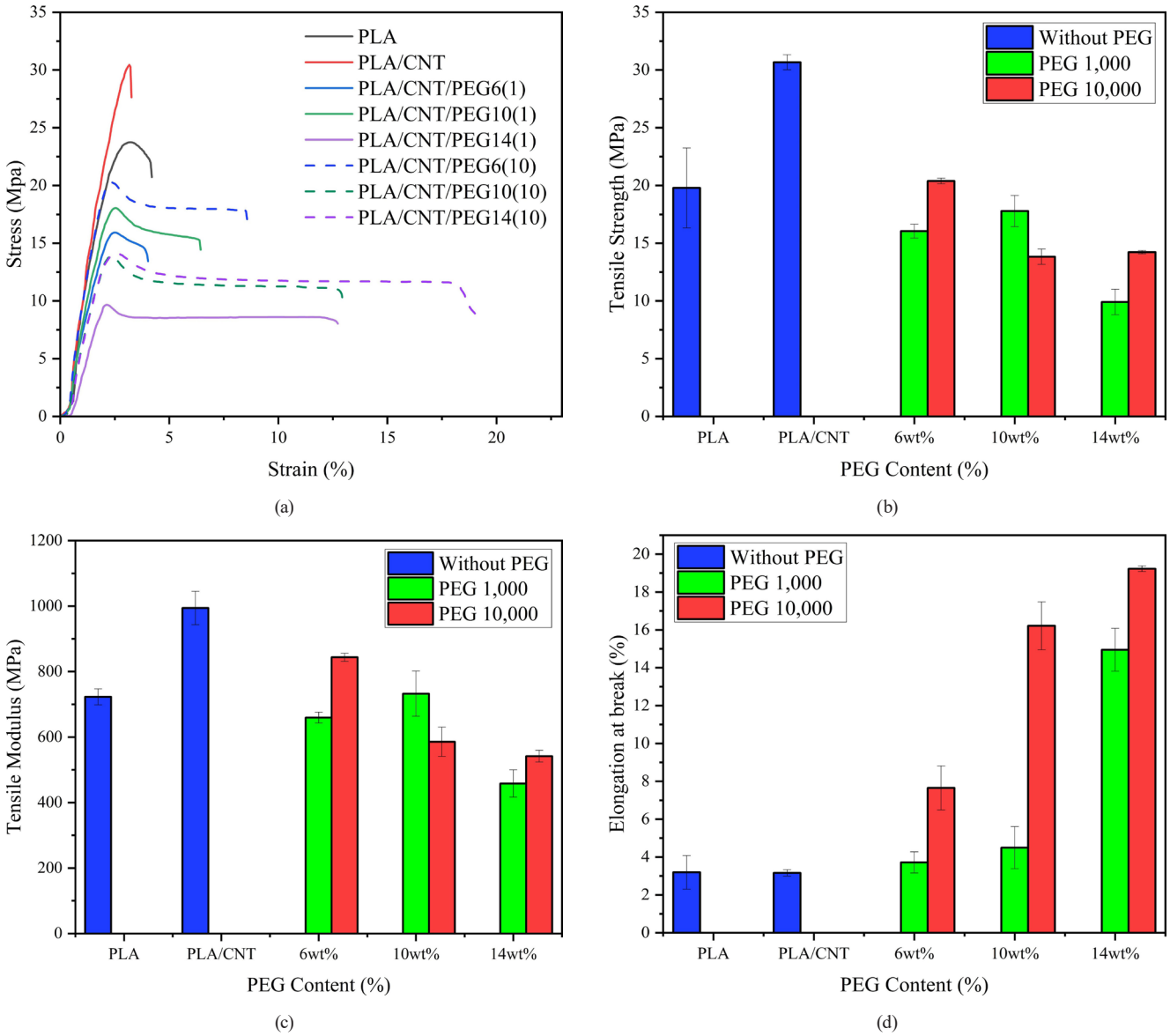

Fig. 3 Tensile properties of PLA, PLA/CNT, and PLA/CNT/PEG composites: (a) typical stress-strain curves, (b) tensile strength, (c) tensile modulus, and (d) elongation at break

modulus of roughly 748.644 MPa. These values align well with the literature, which typically reports PLA tensile strength in the range of 32 ± 5 MPa [27], demonstrating PLA's inherent stiffness and brittleness.

In this study, 8 wt% CNT was added to the composites. Fig. 3 (b) and (c) show that this addition increases the tensile strength and tensile modulus of pure PLA to 30.675 MPa and 994.327 MPa, respectively. As reported in the literature, the presence of carbon nanotubes reduces the mobility and deformability of the PLA matrix, thus increasing rigidity and tensile performance [28]. However, with the inclusion of 6% PEG-1,000 in a PLA/CNT composite, the tensile strength and tensile modulus decrease to 16.051 MPa and 659.721 MPa, respectively. Similar trends are observed with PEG-10,000 as a plasticizer, as illustrated in Fig. 3 (b) and (c). Thus, while PEG enhances elongation at break, it reduces both tensile strength and modulus compared to PLA/CNT.

The addition of PEG as a plasticizer significantly increases the elongation at break while reducing the tensile strength and modulus of the PLA/CNT composite. This trend is observed across a range of PEG additions from 0% to 14 wt%, as shown in Fig. 3 (b), (c), and (d). PEG's plasticizing effect mitigates the brittleness of the PLA/CNT composite, enhancing its flexibility and making it less prone to fracture.

When CNT is uniformly dispersed within the PLA matrix, it significantly enhances the interfacial strength

between the matrix and the filler, reinforcing the composite material [29]. This uniform dispersion allows the effective transfer of applied forces to the CNT, leveraging their inherent strength. The multi-walled structure of CNT contributes to their strong interfacial interaction with the PLA matrix, explaining the observed increase in tensile strength and modulus of PLA/CNT composites. The degree of CNT dispersion within the PLA matrix is further analyzed in the morphological analysis section.

Fig. 3 (d) reveals that the molecular weight of PEG influences the elongation at break of the PLA/CNT composite. Notably, at 14 wt% addition, the elongation at break is longer for composites using PEG-10,000 compared to those using PEG-1,000. This variation can be attributed to the changes in crystallinity and the nature of intermolecular forces between the components of the composite [10, 15]. In this research, the interactions between PLA, CNT, and PEG play a crucial role in determining the mechanical properties. At low PEG concentrations, the strong intermolecular forces between PLA chains dominate, limiting the plasticization effect of PEG. As PEG concentration increases, these similar PLA chain interactions weaken, and the dissimilar intermolecular forces between PLA and PEG become more influential [11, 30]. This results in a composite that becomes more elastic with higher PEG content, as demonstrated by the enhanced elongation at break in Fig. 3 (d).

The observed decrease in tensile strength and modulus with increased PEG content aligns with trends seen in other polymer blends where plasticizers are used to enhance flexibility at the expense of rigidity [31]. However, the significant increase in elongation at break underscores the potential of PLA/CNT/PEG composites for applications requiring flexible, biodegradable materials with moderate conductivity.

3.2 Fourier transform infrared analysis

The chemical structures and molecular interactions of PLA and its composites were investigated using FTIR spectroscopy. Fig. 4 illustrates the effects of PEG concentration and molecular weight on the structural characteristics of the PLA/CNT/PEG blends. The similar IR spectra of the samples indicate that their molecular structures are consistent. The transmittance band data of the samples display typical peaks at 2804–2944 cm^{-1} (C-H stretching) and 841 cm^{-1} ($–CH^2–$ rocking), consistent with previous reports [32, 33].

Several peaks exhibited changes in intensity, namely: 1365–1370 cm^{-1} (C–H bending), 1145–1150 cm^{-1} (–C–O– stretching), 1093–1099 cm^{-1} (–C–O– stretching),

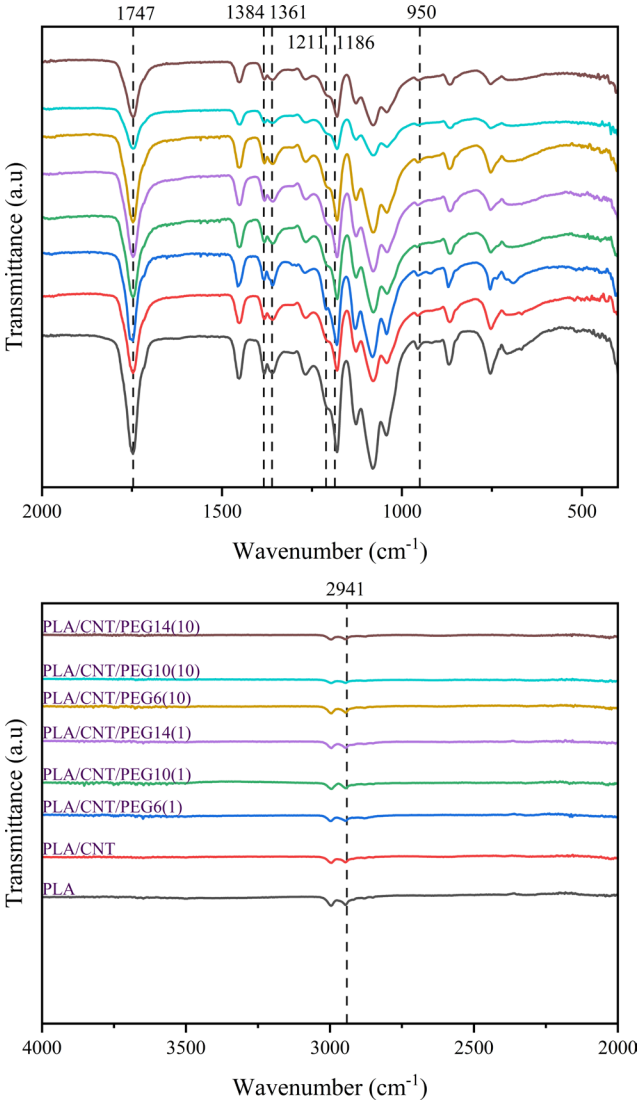

Fig. 4 Comparison of FTIR spectra for PLA, PLA/CNT, and PLA/CNT/PEG composites

960–964 cm^{-1} ($–CH_2$ Gauche rocking), 946–950 cm^{-1} (C–C rocking), and 1748–1746 cm^{-1} (C=O stretching of PLA). The intensity of these wavenumbers becomes weaker as the PEG composition increases, implying significant chemical interactions between PLA and PEG at high PEG concentrations [11]. The interaction between the C=O group in PLA and the –OH group in PEG through strong hydrogen bonding is responsible for the shifting of the C=O stretching peak of PLA (depicted in Fig. 5) [34]. Additionally, the increased elasticity of PLA due to the plasticization effect indicates the presence of some PEG units between the PLA chains [35].

PEG and PLA form strong chemical bonds, facilitating adequate mixing in PLA/CNT composites. Notably, the presence of CNT has relatively no effect on the characteristic peaks of PLA. The distinctive peaks responsible

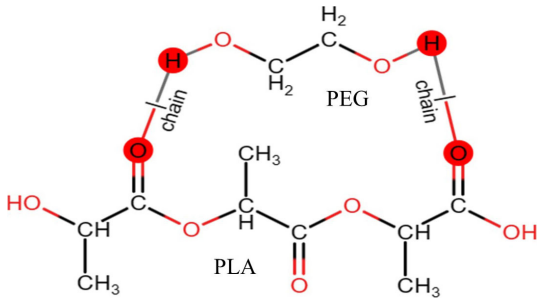

Fig. 5 Possible interaction of PLA with the PEG polymer

for –CH stretching, –C–O– stretching, C–H bending, and C=O stretching were observed across the spectra for all the composites, and no new peaks were formed in the presence of CNT. This suggests that CNT does not introduce new functional groups that could establish a robust interface with the PLA matrix.

The changes in the composites' properties are likely due to physical interactions between the CNT and the PLA/PEG matrix, as well as charge transfer interactions between the conjugated surfaces of the CNT particles and the PLA/PEG [36]. The uniform dispersion of CNT within the matrix enhances these interactions, contributing to the overall mechanical and electrical properties of the composites.

The effects of CNT and PEG incorporation on the amorphous and crystalline phases of PLA are shown in Fig. 6 (a). For the PLA/CNT composite, a decrease in the intensity ratio $I_{1384/1361}$ compared to PLA indicates a decomposition of amorphous PLA. This decrease suggests that the presence of CNT promotes the breakdown of amorphous PLA regions into smaller molecular chains, which in turn facilitates PLA crystallization [37]. With the addition of 6 wt% of PEG-1,000, the $I_{1384/1361}$ intensity ratio decreases further, indicating a continued reduction in amorphous PLA. However, at 10 and 14 wt% PEG-1,000, the ratio shows a slight increase, implying a rise in the amorphous content of PLA. This effect is attributed to PEG's role as a plasticizer, enhancing molecular chain mobility and reducing chain interactions, thus increasing the composite's free volume [38]. This enhanced mobility leads to a more disordered structure, encouraging the transformation from the ordered α' crystalline state to a more amorphous structure [22]. These structural changes correspond to the observed reduction in tensile strength and modulus, with a simultaneous increased flexibility. Similar trends appear for PEG-10,000, with slight increases in amorphous content at 10 and 14 wt%, as seen in Fig. 6 (a).

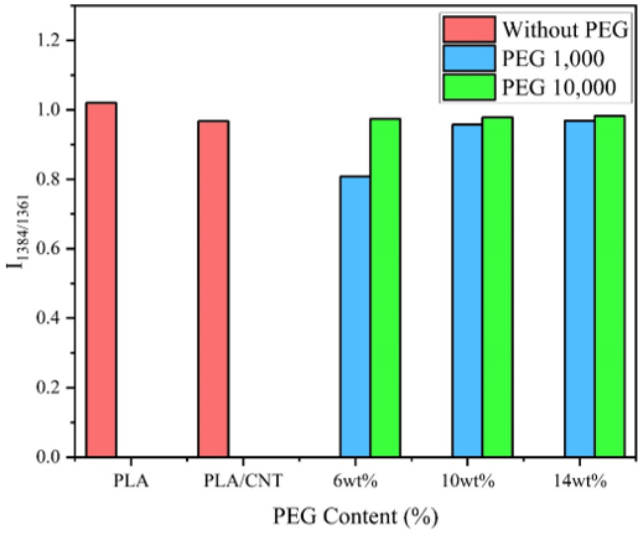

(a)

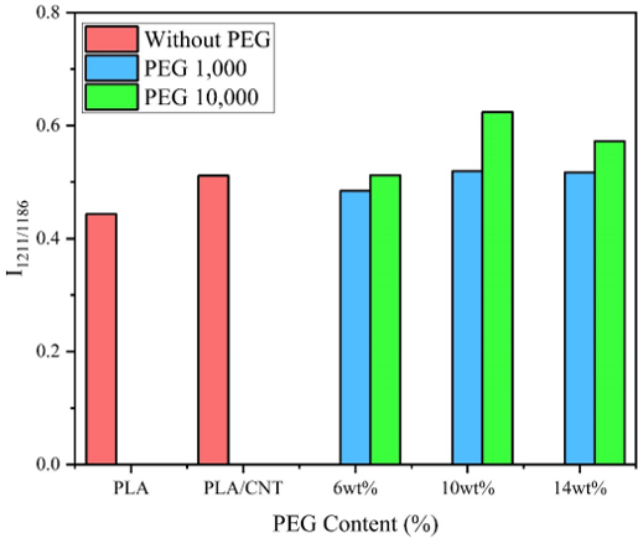

(b)

Fig. 6 The variations of the intensity ratios (a) $I_{1384/1361}$ and (b) $I_{1211/1186}$ of PLA, PLA/CNT, and PLA/CNT/PEG composites

Fig. 6 (b) illustrates the transition between the α and α' crystalline forms in PLA with CNT and PEGs addition. An increase in the intensity ratio $I_{1211/1186}$ reflects an increase in the α crystalline form, signifying the transformation from the α' to α form along with a reduction in amorphous PLA, which raises the overall crystallinity. This transformation correlates with the observed decrease in the $I_{1384/1361}$ ratio for PLA/CNT composite, indicating a reduction in amorphous PLA as the crystallinity rises. The shift from α' to α crystalline structure reduces the flexibility of the PLA composite, which explains the increase in tensile modulus and strength in PLA/CNT. After the addition of 6 wt% of PEGs, the intensity ratio

$I_{1211/1186}$ remained constant. In contrast, the addition of 10 wt% PEGs shows a significant increase in the intensity ratio $I_{1211/1186}$ for PEG-10,000, reflecting an increase in the α crystalline PLA, which raises the crystallinity of the composite. At 14 wt% PEGs, the $I_{1211/1186}$ ratio decreases, suggesting a reverse transformation from the α to the α' PLA, indicating reduced crystallinity. This transition aligns with the observed increase in the $I_{1384/1361}$ reflecting a higher amorphous PLA content in these composites.

The crystallinity index values presented in Table 2 further substantiate these findings, highlighting the critical role of CNT and PEGs in modifying PLA's crystalline structure. The incorporation of CNT notably enhances the degree of crystallinity, increasing the index from 14.12% in pure PLA to 40.85% in PLA/CNT composite, which is consistent with Fig. 6 (a) and (b). This trend continues with PEG addition: at 6 wt% PEGs, crystallinity rises, indicating the combined effects of CNT acting as nucleating agents and PEG's ability to promote molecular mobility. The data further show that, at 10 wt% PEG-10,000, the crystallinity index reaches its peak relative to PEG-1,000, suggesting that PEG-10,000 more effectively interacts with the matrix to enhance crystalline regions. However, with the addition of 14 wt% PEG for both PEG-1,000 and PEG-10,000, the crystallinity index decreases slightly. This decrease likely results from the increased plasticizing effect of PEG at higher concentrations, which leads to greater chain mobility and disrupts crystalline structure. Supporting these observations, previous studies have shown that differential scanning calorimetry (DSC) revealed that incorporating 14 wt% of PEG 10,000 into PLA/MWCNT composite significantly enhances the melting enthalpy (ΔH_m) from 18.3 J g^{-1} to 24.6 J g^{-1} and the degree of crystallinity from 2% to 17.3% [39]. This crystallinity increase is particularly significant at lower CNT concentration (1 wt%), indicating that PEG's plasticizing effect, combined with CNT, can effectively modulate the crystalline structure of PLA.

Table 2 Changes in the overall crystallinity index of PLA and CPCs

Sample	x_{IF}
PLA	14.12%
PLA/CNT	40.85%
PLA/CNT/PEG6 (1)	44.20%
PLA/CNT/PEG10 (1)	46.55%
PLA/CNT/PEG14 (1)	45.12%
PLA/CNT/PEG6 (10)	45.71%
PLA/CNT/PEG10 (10)	47.25%
PLA/CNT/PEG14 (10)	46.79%

The FTIR analysis provides crucial insights into the molecular interactions and structure within the PLA/CNT/PEG composites. The weakening of specific peaks with increased PEG content highlights the significant role of PEG in modifying the composite structure. The hydrogen bonding between PLA and PEG, indicated by the shift in the C=O stretching peak, underscores the importance of chemical interactions in determining the composite properties. Furthermore, the physical and charge transfer interactions between CNT and the PLA/PEG matrix explain the enhanced mechanical and electrical properties observed in these composites. These interactions can improve CNT dispersion within the matrix, facilitating stress transfer and conductive pathways, which ultimately lead to the increased flexibility and electrical conductivity of the composites.

3.3 Morphological properties

The examination of the morphological elements is crucial for understanding the physical properties of the resulting blends. Fig. 7 shows SEM micrographs of the sample surface at a magnification of 1,000×. Neat PLA exhibits a smooth fracture surface due to its brittle and stiff behavior. A relatively uniform distribution and dispersion of CNT in the PLA matrix can be observed in Fig. 7 (b), (c), and (d).

The use of an ultrasonic homogenizer to stir a solution of PLA/CNT/PEG results in a reasonable CNT distribution in the PLA matrix. The solvent casting of PLA in chloroform, accompanied by ultrasonic stirring, creates high shear stress on the PLA solution, resulting in an equal and uniform dispersion of CNT in PLA [40]. Proper CNT dispersion is crucial as it enhances the bonding interactions between the polymer molecules and the CNT fillers, potentially improving the composite's mechanical and electrical properties. The FTIR spectra presented in Fig. 4 show slight changes in the spectrum of PLA after the incorporation of CNT, indicating modifications in the molecular interactions within the composite structure.

The distribution and dispersion of fillers and plasticizers significantly impact the crystallinity and amorphous regions of PLA. Several studies have highlighted that well-dispersed CNT fillers can act as a nucleating agent, enhancing the crystallinity of the composites [41, 42]. The addition of CNT, known for its role as a nucleating agents, has been shown to increase the degree of crystallinity in PLA/CNT. This increase is often associated with a smooth fracture surface and uniform composite morphology, indicating strong interactions between the CNT and the PLA matrix. Additionally, Fig. 6 (a) and (b) show that incorporating CNT with 6 and 10 wt% PEGs results

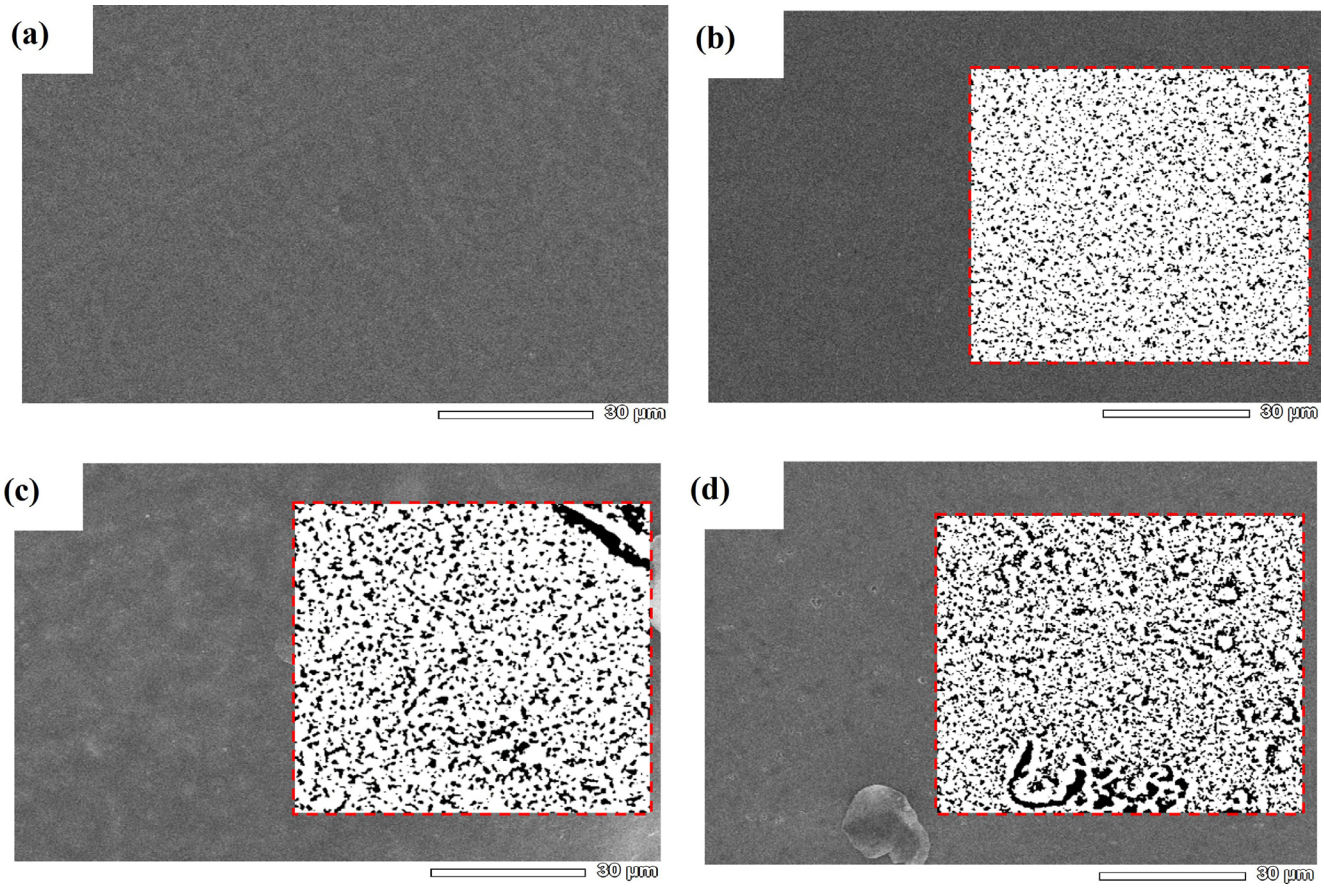

Fig. 7 SEM micrographs of samples at 1,000× magnification: (a) PLA, (b) PLA/CNT, (c) PLA/CNT/PEG10 (1), and (d) PLA/CNT/PEG10 (10). The inset images depict the dispersion of CNT in the matrix

in increased crystallinity, as indicated by the observed decrease in the intensity ratio $I_{1384/1361}$ and increase in the intensity ratio $I_{1211/1186}$. This shift reflects a reduction in amorphous PLA and an increase in the α crystalline form, contributing to overall crystallinity, as shown in Table 2. However, at 14 wt% PEGs, the crystallinity decreases, suggesting that PEG's plasticizing effect enhances molecular mobility and reduces chain interactions, disrupting crystalline regions and promoting a more amorphous structure.

To investigate the effect of PEG on CNT dispersion more precisely, the diameter of the CNT agglomerations (the surrounding circle around each cluster) was measured from the total number of aggregations in each composite sample using ImageJ software [43]. Fig. 8 depicts the findings of this analysis. The average agglomeration diameter (D_{ave}) is highly dependent on PEG. D_{ave}'s value decreased after combining with PEGs. The agglomeration diameter of PLA/CNT composite without PEG is broad, measuring approximately 207 nm. However, upon the inclusion of PEGs, the size distribution narrows and shifts to smaller values, decreasing to 78 nm for PEG-1,000 and further to 63 nm for PEG-10,000. This reduction in agglomeration size indicates improved CNT dispersion within the PLA matrix, with PEG-10,000 exhibiting superior dispersing capability compared to PEG-1,000. These findings align with the crystallinity trends observed in Fig. 6 (b) and Table 2; the crystallinity is higher in the 10 wt% PEG-10,000 composite than in PEG-1,000 due to improved CNT dispersion.

Elemental analysis offers a promising approach for monitoring the purification process of composites. As illustrated in Fig. 9, the EDX spectrum reveals distinct signals corresponding to the elemental composition of PLA, PLA/CNT, and PLA/CNT/PEG. The highlighted red square delineates the scanned spectrum area. The accompanying table provides insights into the relative mass fraction and atomic percentage of carbon and oxygen in PLA/CNT, both before and after incorporating PEG. Notably, the presence of metallic impurities, such as copper and zinc, is indicated at trace levels. Additionally, traces of solvent, notably chlorine, are detected in each sample.

3.4 Electrical properties

Electrically insulating materials are characterized by a ρ_v greater than 10^{11} Ω cm, which impedes electron flow across their surfaces. In contrast, antistatic and dissipative materials exhibit volume resistivities ranging from

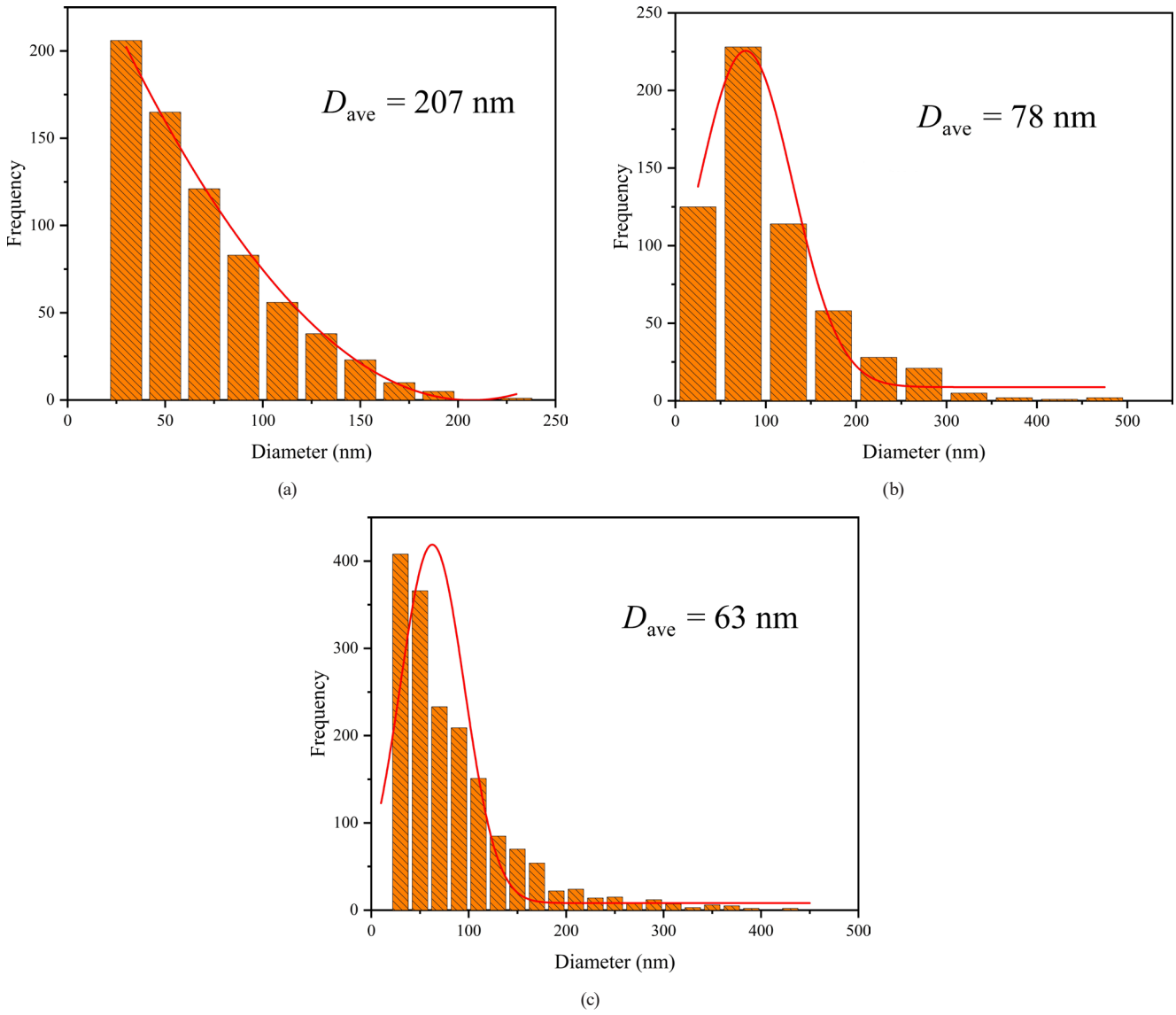

Fig. 8 Diameter distribution of CNT in (a) PLA/CNT, (b) PLA/CNT/PEG10 (1), and (c) PLA/CNT/PEG10 (10) composites

10^4 to 10^{11} Ω cm, facilitating electronic conduction [1, 44]. As depicted in Fig. 10 (a), PLA/CNT and PLA/CNT/PEG composites fall within the category of antistatic and dissipative materials, making these composites suitable for antistatic packaging.

The electrical properties of PLA composites are highly dependent on the presence of conductive fillers (CNT) and the morphology of the resulting polymer composites [45]. Fig. 10 (a) depicts the specific resistivity of PLA and PLA/CNT with different concentrations of PEG. It was discovered that neat PLA had a resistivity of 3.94×10^{19} Ω cm, rendering it an electrical insulator, similar to the majority of polymers. However, with a CNT composition of 8 wt%, the electrical resistivity decreases to 5.32×10^{10} Ω cm, or the electrical conductivity reaches 1.89×10^{-11} S cm^{-1} (Fig. 10 (b)). Furthermore, with the addition of 10 wt% PEG-1,000 and PEG-10,000, the electrical resistivity decreases to as low as 1.54×10^9 Ω cm and 1.40×10^9 Ω cm, respectively. The optimal outcome is achieved with the addition of 14 wt% PEG-10,000. This phenomenon demonstrates how increasing the PEG concentration in PLA/CNT can promote the development of charge distribution and permeable conduction pathways on the composite surface, thereby improving the electrical conductivity [15].

The investigation into the impact of technological variables on electrical resistivity revealed that under conducive conditions, selecting a lower filling velocity, higher liquefier temperature, and larger layer thickness is advantageous for achieving minimal resistivity targets [15]. However, this research utilized thinner film thicknesses, typically ranging from 0.04 to 0.1 mm, yielded poorer resistivity results compared to other research on PLA/CNT composites produced by melt blending and additional FDM process, which exhibited resistivity as low as 1×10^4 Ω cm

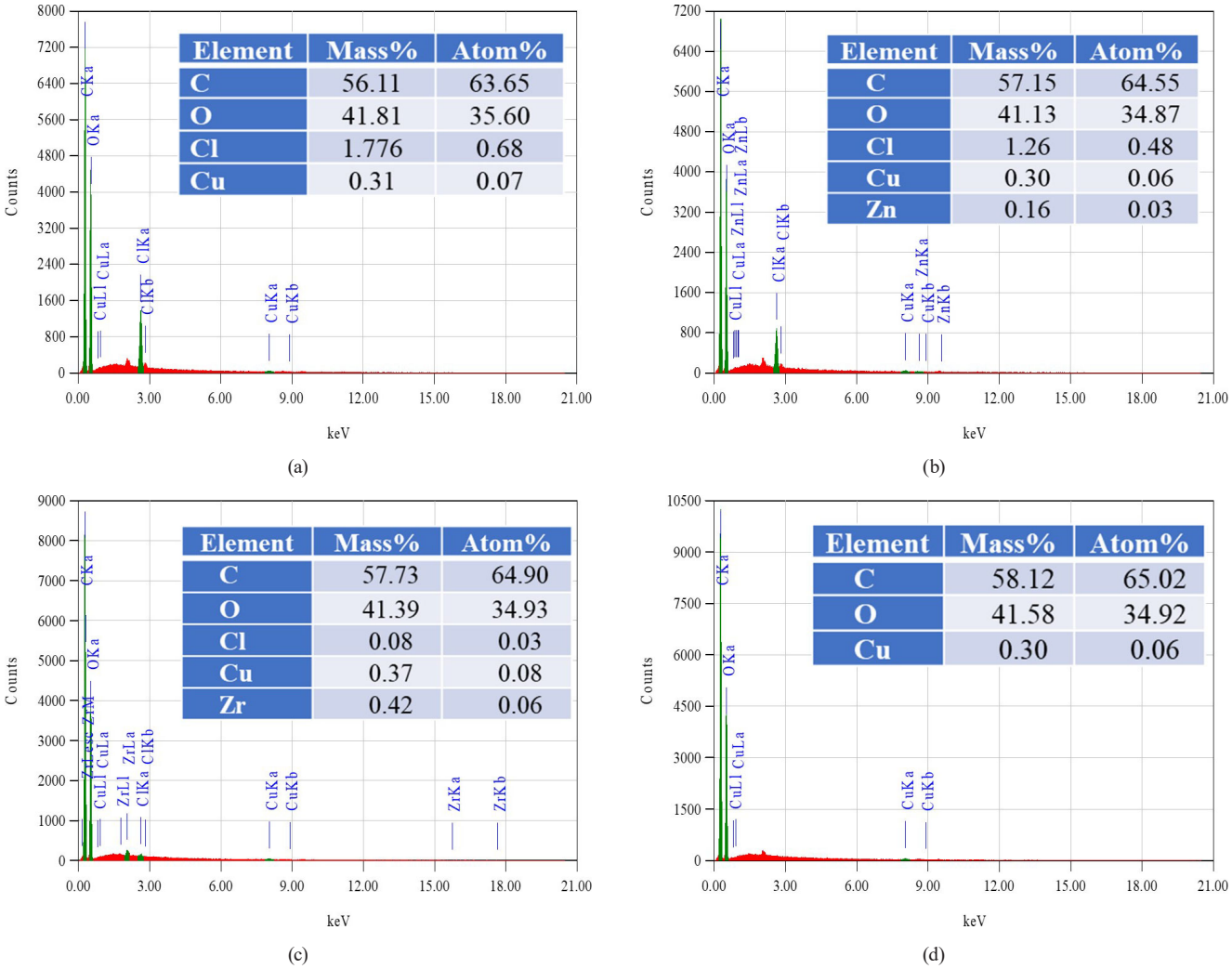

Fig. 9 EDX Analysis of SEM Micrographs: (a) PLA (b) PLA/CNT (c) PLA/CNT/PEG10 (1) (d) PLA/CNT/PEG10 (10)

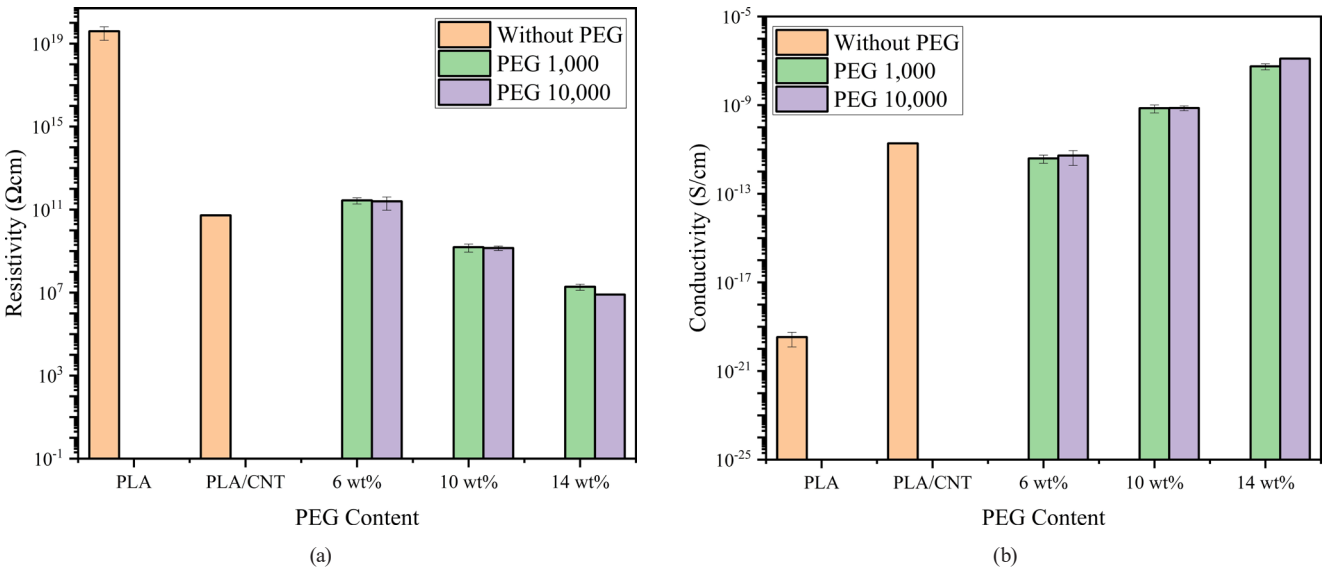

Fig. 10 Electrical properties of PLA, PLA/CNT, and PLA/CNT/PEG composites: (a) resistivity and (b) conductivity

(8 wt% CNT, 0.3 mm film thickness) [15]. This disparity underscores the importance of film thickness in determining electrical properties. Furthermore, employing a lower liquefier temperature of 55 °C for casting to form the film supports these findings.

In addition to matrix properties such as crystallinity, the interparticle distance between conducting fillers in a given polymer matrix influences conductivity. One-dimensional nanofillers such as CNT can achieve low electrical percolation thresholds due to the high aspect ratios of their nanoparticles [3]. Moreover, Fig. 8 demonstrates that the agglomeration diameter distribution narrows and shifts to lower values with the addition of PEG to the PLA/CNT composite. This is attributed to the accelerated crystallization of PLA, which is facilitated by the plasticizing role of PEG. Nonetheless, the crystallization of PEG is slowed due to the increased rigidity of the system caused by PLA crystallization [46]. This increases the distance between conducting fillers (CNT) in the PLA matrix, allowing faster segmental movement of the polymer backbone, resulting in more free volume, which promotes ionic movement through the host matrix and subsequently increases conductivity [47, 48].

4 Conclusion

A solvent-casting process was used to investigate the effect of CNT and PEG on the properties of CPCs based on PLA. The mechanical characteristics indicate that the addition of CNT reinforces the PLA matrix, enhancing its strength and modulus. In contrast, PEG serves as a plasticizer, improving flexibility while reducing rigidity. The interplay between CNT and PEG within the PLA matrix allows for tailoring the mechanical properties of the composite to meet specific application requirements. FTIR spectroscopy analysis reveals that PEG significantly influences the chemical structure and interactions within PLA/CNT composite, enhancing their mechanical flexibility and electrical conductivity. The lack of new peaks in the presence of CNT indicates that physical and charge transfer interactions, rather than chemical bonding, are responsible for the observed changes in composite properties. The conformational changes and order states of PLA in the composites are tracked using the intensity ratios of the band pairs 1384/1361 cm^{-1} and 1211/1186 cm^{-1} of FTIR spectra. Monitoring the intensity ratios $I_{1384/1361}$ and $I_{1211/1186}$ reveals two key transitions:

1. Between amorphous and crystalline PLA.
2. Between the α and α' crystalline forms of PLA.

These transitions are identified through the distinct variation trends in the respective intensity ratios, providing insight into the structural modifications occurring within the composite. According to the SEM results, the fracture surface of PLA/CNT/PEG is homogeneous and uniform. A high level of nanofiller dispersion in the composite results in improved electrical properties. The electrical properties of PLA/CNT/PEG were highly dependent on the concentration of PEG. At the same CNT concentration, the electrical conductivity increased after the incorporation of PEG. PEG aids in the dispersion of CNT within the polymer matrix, leading to an increase in electrical conductivity. The addition of PEG to PLA/CNT composites not only improves their mechanical flexibility but also enhances their electrical conductivity, making them suitable for applications such as antistatic packaging. The results demonstrate the potential of tailoring the properties of PLA-based composites through the strategic addition of conductive fillers and plasticizers.

Acknowledgment

The Indonesian Government financially supported this research through the Ministry of Education, Culture, Research and Technology of Indonesia through the "Penelitian Dasar Unggulan Perguruan Tinggi 2023", contract number 380.1/UN27.22/PT.01.03/2023.

References

[1] de Souza Vieira, L., dos Anjos, E. G. R., Verginio, G. E. A., Oyama, I. C., Braga, N. F., da Silva, T. F., Montagna, L. S., Rezende, M. C., Passador, F. R. "Carbon-based materials as antistatic agents for the production of antistatic packaging: a review", Journal of Materials Science: Materials in Electronics, 32(4), pp. 3929–3947, 2021. https://doi.org/10.1007/s10854-020-05178-6

[2] Srihata, W., Jamnongkan, T., Rattanasak, U., Boonsang, S., Kaewpirom, S. "Enhanced electrostatic dissipative properties of chitosan/gelatin composite films filled with reduced graphene oxide", Journal of Materials Science: Materials in Electronics, 28(1), pp. 999–1010, 2017. https://doi.org/10.1007/s10854-016-5620-0

[3] Ramanujam, B. T. S., Annamalai, P. K. "1 - Conducting polymer-graphite binary and hybrid composites: Structure, properties, and applications", In: Thakur, V. K., Thakur, M. K., Pappu, A. (eds.) Hybrid Polymer Composite Materials: Applications, Woodhead Publishing, 2017, pp. 1–34. ISBN 978-0-08-100785-3 https://doi.org/10.1016/B978-0-08-100785-3.00001-2

[4] Ke, F., Song, F., Zhang, H., Xu, J., Wang, H., Chen, Y. "Layer-by-layer assembly for all-graphene coated conductive fibers toward superior temperature sensitivity and humidity independence", Composites Part B: Engineering, 200, 108253, 2020. https://doi.org/10.1016/J.COMPOSITESB.2020.108253

[5] Yang, X., Fan, S., Li, Y., Guo, Y., Li, Y., Ruan, K., Zhang, S., Zhang, J., Kong, J., Gu, J. "Synchronously improved electromagnetic interference shielding and thermal conductivity for epoxy nanocomposites by constructing 3D copper nanowires/thermally annealed graphene aerogel framework", Composites Part A: Applied Science and Manufacturing, 128, 105670, 2020. https://doi.org/10.1016/j.compositesa.2019.105670

[6] Guo, Y., Zuo, X., Xue, Y., Tang, J., Gouzman, M., Fang, Y., Zhou, Y., Wang, L., Yu, Y., Rafailovich, M. H. "Engineering thermally and electrically conductive biodegradable polymer nanocomposites", Composites Part B: Engineering, 189, 107905, 2020. https://doi.org/10.1016/j.compositesb.2020.107905

[7] Huang, J., Mao, C., Zhu, Y., Jiang, W., Yang, X. "Control of carbon nanotubes at the interface of a co-continuous immiscible polymer blend to fabricate conductive composites with ultralow percolation thresholds", Carbon, 73, pp. 267–274, 2014. https://doi.org/10.1016/J.CARBON.2014.02.063

[8] Feng, X., Wang, X., Cai, W., Qiu, S., Hu, Y., Liew, K. M. "Studies on Synthesis of Electrochemically Exfoliated Functionalized Graphene and Polylactic Acid/Ferric Phytate Functionalized Graphene Nanocomposites as New Fire Hazard Suppression Materials", ACS Applied Materials & Interfaces, 8(38), pp. 25552–25562, 2016. https://doi.org/10.1021/acsami.6b08373

[9] Farah, S., Anderson, D. G., Langer, R. "Physical and mechanical properties of PLA, and their functions in widespread applications — A comprehensive review", Advanced Drug Delivery Reviews, 107, pp. 367–392, 2016. https://doi.org/10.1016/j.addr.2016.06.012

[10] Athanasoulia, I.-G., Tarantili, P. A. "Preparation and characterization of polyethylene glycol/poly(L-lactic acid) blends", Pure and Applied Chemistry, 89(1), pp. 141–152, 2017. https://doi.org/10.1515/pac-2016-0919

[11] Shin, H., Thanakkasaranee, S., Sadeghi, K., Seo, J. "Preparation and Characterization of Ductile PLA/PEG Blend Films for Eco-Friendly Flexible Packaging Application", 34, pp. 1–29, 2022. https://doi.org/10.2139/ssrn.4164380

[12] Ali, F., Awale, R. J., Saeed Mirghani, M. E., Anuar, H., Samat, N. "Preparation and characterization of plasticized polylactic acid/starch blend", Jurnal Teknologi, 78(11–2), pp. 7–12, 2016. https://doi.org/10.11113/jt.v78.9936

[13] Earp, B., Dunn, D., Phillips, J., Agrawal, R., Ansell, T., Aceves, P., De Rosa, I., Xin, W., Luhrs, C. "Enhancement of electrical conductivity of carbon nanotube sheets through copper addition using reduction expansion synthesis", Materials Research Bulletin, 131, 110969, 2020. https://doi.org/10.1016/j.materresbull.2020.110969

[14] Cao, Q., Yu, Q., Connell, D. W., Yu, G. "Titania/carbon nanotube composite (TiO_2/CNT) and its application for removal of organic pollutants", Clean Technologies and Environmental Policy, 15(6), pp. 871–880, 2013. https://doi.org/10.1007/s10098-013-0581-y

[15] Yang, L., Li, S., Zhou, X., Liu, J., Li, Y., Yang, M., Yuan, Q., Zhang, W. "Effects of carbon nanotube on the thermal, mechanical, and electrical properties of PLA/CNT printed parts in the FDM process", Synthetic Metals, 253, pp. 122–130, 2019. https://doi.org/10.1016/j.synthmet.2019.05.008

[16] Alipour, A., Giffney, T., Lin, R., Jayaraman, K. "Effects of matrix viscosity on morphological and rheological properties and the electrical percolation threshold in graphene/epoxy nanocomposites", eXPRESS Polymer Letters, 15(6), pp. 541–553, 2021. https://doi.org/10.3144/expresspolymlett.2021.46

[17] Sanatgar, R. H., Cayla, A., Campagne, C., Nierstrasz, V. "Morphological and electrical characterization of conductive polylactic acid based nanocomposite before and after FDM 3D printing", Journal of Applied Polymer Science, 136(6), 47040, 2019. https://doi.org/10.1002/app.47040

[18] Petrény, R., Tóth, C., Horváth, A., Mészáros, L. "Development of electrically conductive hybrid composites with a poly(lactic acid) matrix, with enhanced toughness for injection molding, and material extrusion-based additive manufacturing", Heliyon, 8(8), e10287, 2022. https://doi.org/10.1016/j.heliyon.2022.e10287

[19] Sharma, S., Singh, A. A., Majumdar, A., Butola, B. S. "Tailoring the mechanical and thermal properties of polylactic acid-based bionanocomposite films using halloysite nanotubes and polyethylene glycol by solvent casting process", Journal of Materials Science, 54(12), pp. 8971–8983, 2019. https://doi.org/10.1007/s10853-019-03521-9

[20] ASTM "ASTM D882-10, Standard Test Methods for Tensile Properties of Thin Plastic Sheeting", ASTM International, West Conshohocken, PA, USA, 2012. https://doi.org/10.1520/D0882-10

[21] Chalid, M., Gustiraharjo, G., Pangesty, A. I., Adyandra, A., Whulanza, Y., Supriadi, S. "Effect of PEG Incorporation on Physicochemical and *in vitro* Degradation of PLLA/PDLLA Blends: Application in Biodegradable Implants", Journal of Renewable Materials, 11(7), pp. 3043–3056, 2023. https://doi.org/10.32604/jrm.2023.026788

[22] Dou, T., Zhou, B., Hu, S., Zhang, P. "Evolution of the structural polymorphs of poly(L-lactic acid) during the in vitro mineralization of its hydroxyapatite nanocomposites by attenuated total reflection fourier transform infrared mapping coupled with principal component analysis", Polymer, 236, 124318, 2021. https://doi.org/10.1016/j.polymer.2021.124318

[23] Giełdowska, M., Puchalski, M., Sztajnowski, S., Krucińska, I. "Evolution of the Molecular and Supramolecular Structures of PLA during the Thermally Supported Hydrolytic Degradation of Wet Spinning Fibers", Macromolecules, 55(22), pp. 10100–10112, 2022. https://doi.org/10.1021/acs.macromol.2c01778

[24] Pan, L., Lv, Q., Xu, N. "Properties and mechanism of antistatic biodegradable polylactic acid/multi-walled carbon nanotube composites", Journal of Engineered Fibers and Fabrics, 15, 1558925020968813, 2020. https://doi.org/10.1177/1558925020968813

[25] Silva, T. F. d., Menezes, F., Montagna, L. S., Lemes, A. P., Passador, F. R. "Preparation and characterization of antistatic packaging for electronic components based on poly(lactic acid)/carbon black composites", Journal of Applied Polymer Science, 136(13), 47273, 2019. https://doi.org/10.1002/app.47273

[26] Auras, R., Lim, L.-T., Selke, S. E. M., Tsuji, H. "Poly(Lactic Acid): Synthesis, Structures, Properties, Processing, and Applications", John Wiley & Sons, Inc., 2010. ISBN 9780470293669 https://doi.org/10.1002/9780470649848

[27] De Bortoli, L. S., de Farias, R., Mezalira, D. Z., Schabbach, L. M., Fredel, M. C. "Functionalized carbon nanotubes for 3D-printed PLA-nanocomposites: Effects on thermal and mechanical properties", Materials Today Communications, 31, 103402, 2022. https://doi.org/10.1016/j.mtcomm.2022.103402

[28] Leal, C. V., Martinez, D. S. T., Más, B. A., Alves, O. L., Duek, E. A. R. "Influence of purified multiwalled carbon nanotubes on the mechanical and morphological behavior in poly (L-lactic acid) matrix", Journal of the Mechanical Behavior of Biomedical Materials, 59, pp. 547–560, 2016. https://doi.org/10.1016/j.jmbbm.2016.03.016

[29] Park, S. H., Lee, S. G., Kim, S. H. "Isothermal crystallization behavior and mechanical properties of polylactide/carbon nanotube nanocomposites", Composites Part A: Applied Science and Manufacturing, 46, pp. 11–18, 2013. https://doi.org/10.1016/j.compositesa.2012.10.011

[30] Li, F.-J., Tan, L.-C., Zhang, S.-D., Zhu, B. "Compatibility, steady and dynamic rheological behaviors of polylactide/poly(ethylene glycol) blends", Journal of Applied Polymer Science, 133(4), 42919, 2016. https://doi.org/10.1002/app.42919

[31] Wang, S.-F., Wu, Y.-C., Cheng, Y.-C., Hu, W.-W. "The Development of Polylactic Acid/Multi-Wall Carbon Nanotubes/Polyethylene Glycol Scaffolds for Bone Tissue Regeneration Application", Polymers, 13(11), 1740, 2021. https://doi.org/10.3390/polym13111740

[32] Chieng, B. W., Ibrahim, N. A., Yunus, W. M. Z. W., Hussein, M. Z., Then, Y. Y., Loo, Y. Y. "Effects of Graphene Nanoplatelets and Reduced Graphene Oxide on Poly(lactic acid) and Plasticized Poly(lactic acid): A Comparative Study", Polymers, 6(8), pp. 2232–2246, 2014. https://doi.org/10.3390/polym6082232

[33] Chieng, B. W., Azowa, I. N., Wan Yunus, W. M. Z., Hussein, M. Z. "Effects of Graphene Nanopletelets on Poly(Lactic Acid)/Poly(Ethylene Glycol) Polymer Nanocomposites", Advanced Materials Research, 1024, pp. 136–139, 2014. https://doi.org/10.4028/www.scientific.net/AMR.1024.136

[34] Sundar, N., Stanley, S. J., Kumar, S. A., Keerthana, P., Kumar, G. A. "Development of dual purpose, industrially important PLA–PEG based coated abrasives and packaging materials", Journal of Applied Polymer Science, 138(21), 50495, 2021. https://doi.org/10.1002/app.50495

[35] Ahmed, H. T., Jalal, V. J., Tahir, D. A., Mohamad, A. H., Abdullah, O. G. "Effect of PEG as a plasticizer on the electrical and optical properties of polymer blend electrolyte MC-CH-$LiBF_4$ based films", Results in Physics, 15, 102735, 2019. https://doi.org/10.1016/j.rinp.2019.102735

[36] Ahmad, A. F., Aziz, S. A., Obaiys, S. J., Zaid, M. H. M., Matori, K. A., Samikannu, K., Aliyu, U. S. "Biodegradable Poly (lactic acid)/Poly (ethylene glycol) Reinforced Multi-Walled Carbon Nanotube Nanocomposite Fabrication, Characterization, Properties, and Applications", Polymers, 12(2), 427, 2020. https://doi.org/10.3390/polym12020427

[37] Beltrán, F. R., de la Orden, M. U., Lorenzo, V., Pérez, E., Cerrada, M. L., Martínez Urreaga, J. "Water-induced structural changes in poly(lactic acid) and PLLA-clay nanocomposites", Polymer, 107, pp. 211–222, 2016. https://doi.org/10.1016/j.polymer.2016.11.031

[38] Wang, S., Wu, R., Zhang, J., Leng, Y., Li, Q. "PLA/PEG/MWCNT composites with improved processability and mechanical properties", Polymer-Plastics Technology and Materials, 60(4), pp. 430–439, 2021. https://doi.org/10.1080/25740881.2020.1811324

[39] Rifa'i, A. F., Kaavessina, M., Distantina, S. "Evaluation of the Chemical Structure and Thermal Properties of Polyethylene Glycol (PEG)-Doped Polylactic Acid (PLA)/Multiwalled Carbon Nanotube (MWCNT) Composites", Indonesian Journal of Chemical Analysis (IJCA), 7(2), pp. 66–76, 2024. https://doi.org/10.20885/ijca.vol7.iss2.art5

[40] Park, S. G., Abdal-Hay, A., Lim, J. K. "Biodegradable poly(lactic acid)/multiwalled carbon nanotube nanocomposite fabrication using casting and hot press techniques", Archives of Metallurgy and Materials, 60(2), pp. 1557–1559, 2015. https://doi.org/10.1515/amm-2015-0172

[41] Norazlina, H., Suhaila, A., Nabihah, A., Rabiatul, M. M., Zulhelmie, I., Yusoh, Y. "Degradation behaviour of plasticized PLA/CNTs nanocomposites prepared by the different technique of blending", IOP Conference Series: Materials Science and Engineering, 2021, 012002, 2021. https://doi.org/10.1088/1757-899x/1068/1/012002

[42] Norazlina, H., Kamal, Y. "Elucidating the plasticizing effect on mechanical and thermal properties of poly(lactic acid)/carbon nanotubes nanocomposites", Polymer Bulletin, 78(12), pp. 6911–6933, 2021. https://doi.org/10.1007/s00289-020-03471-2

[43] Wayne Rasband and contributors National Institutes of Health, USA "ImageJ software, (1.54d)", [computer program] Available at: https://imagej.net/ij/docs/index.html [Accessed: 12 March 2024]

[44] Pang, H., Xu, L., Yan, D.-X., Li, Z.-M. "Conductive polymer composites with segregated structures", Progress in Polymer Science, 39(11), pp. 1908–1933, 2014. https://doi.org/10.1016/j.progpolymsci.2014.07.007

[45] Chen, J., Shi, Y.-Y., Yang, J.-H., Zhang, N., Huang, T., Chen, C., Wang, Y., Zhou, Z.-W. "A simple strategy to achieve very low percolation threshold *via* the selective distribution of carbon nanotubes at the interface of polymer blends", Journal of Materials Chemistry, 22(42), pp. 22398–22404, 2012. https://doi.org/10.1039/c2jm34295b

[46] Nofar, M., Sacligil, D., Carreau, P. J., Kamal, M. R., Heuzey, M. C. "Poly (lactic acid) blends: Processing, properties and applications", International Journal of Biological Macromolecules, 125, pp. 307–360, 2019. https://doi.org/10.1016/j.ijbiomac.2018.12.002

[47] Perumal, P., Christopher Selvin, P., Selvasekarapandian, S., Sivaraj, P., Abhilash, K. P., Moniha, V., Manjula Devi, R. "Plasticizer incorporated, novel eco-friendly bio-polymer based solid bio-membrane for electrochemical clean energy applications", Polymer Degradation and Stability, 159, pp. 43–53, 2019. https://doi.org/10.1016/j.polymdegradstab.2018.11.013

[48] Naiwi, T. S. R. T., Aung, M. M., Ahmad, A., Rayung, M., Su'ait, M. S., Yusof, N. A., Lae, K. Z. W. "Enhancement of Plasticizing Effect on Bio-Based Polyurethane Acrylate Solid Polymer Electrolyte and Its Properties", Polymers, 10(10), 1142, 2018. https://doi.org/10.3390/polym10101142